Journal of Asian Ceramic Societies 3 (2015) 255–261

Journal of Asian Ceramic Societies

journal homepage: www.elsevier.com/locate/jascer

The crystallization behaviour and bioactivity of wollastonite glass-ceramic based on $Na_2O–K_2O–CaO–SiO_2–F$ glass system

S.M. Salman, S.N. Salama, H.A. Abo-Mosallam *

Glass Research Department, National Research Centre, Dokki, Cairo, Egypt

ARTICLE INFO

Article history:
Received 8 March 2015
Received in revised form 22 April 2015
Accepted 28 April 2015
Available online 20 May 2015

Keywords:
Glass
Crystallization
Glass-ceramics
Wollastonite
Biomaterials

ABSTRACT

The study concerns about the crystallization behaviour and in vitro bioactivity of a glass-ceramic prepared from a series of glasses in the $Na_2O–K_2O–CaO–SiO_2–F$ system. A minor amount of cerium oxide was also added instead of calcium oxide in some selective glass batches. The main crystalline phases, formed after the appropriate heat treatments, were wollastonite solid solution and pseudo-wollastonite-like phases. There is a preferential tendency for wollastonite ($CaSiO_3$) to accommodate K, Na, F, and Ce ions in its structure forming wollastonite solid solution with variable formulas. The bioactivity of the resulting crystalline materials was examined in vitro by immersion in simulated body fluid at 37 °C. An increase of the surface bioactivity of glass-ceramic with the Na_2O/K_2O replacement was observed which is attributed to the augmentation solubility of the crystalline sample. On the other hand, the bioactivity of the crystalline sample with CeO_2/CaO replacement was improved by the crystallization of pseudo-wollastonite phase together with wollastonite solid solution phase.

1. Introduction

Glass-ceramics are produced by controlled nucleation and crystallization of glasses. The great varieties of compositions and microstructures with specific technological properties have allowed glass-ceramics to be used in a wide range of applications [1]. There is great interest in glass-ceramics that possess appropriate physical, mechanical, and biological properties for biomedical applications. These materials should be biocompatible and in most cases bioactive. Bioactivity is defined as the ability of biomaterials to promote the formation of a crystalline hydroxyl apatite (HA) layer from physiological fluid [2]. In implantology, there is considerable interest in bioactive materials to establish strong chemical bonding between the implant and bone, as well as to accelerate implant anchorage by inducing an HA layer on the implant surface [3]. Currently, several bioactive glass-ceramics are used for clinical applications as middle-ear implant for the reconstruction of the iliac crest and also as vertebral prostheses or dental implants [4].

Wollastonite ($CaSiO_3$) or calcium metasilicate is a chain silicate mineral. As it is known, calcium silicate has mainly two normal modifications, one is the low temperature phase wollastonite and the other is the high temperature phase pseudo-wollastonite [5]. By heating over 1125 °C, during the sintering, the low temperature form of wollastonite transformed reconstructively into pseudo-wollastonite [6]. Since the 1990s, wollastonite ($CaSiO_3$) ceramics have been studied as biomaterials for artificial bones and dental roots because wollastonite exhibits good bioactivity and biocompatibility. Some investigators have reported that wollastonite and pseudo-wollastonite ceramics are bioactive and observed that the formation of apatite on $CaSiO_3$ ceramics is faster than that on other bioglass and glass-ceramics in simulated body fluids (SBF) [5]. Siriphannon et al. [7] have found that the rate of hydroxyapatite (HA) formation on pure $CaSiO_3$ ceramic surface was faster than that on the biocompatible apatite wollastonite A/W glass-ceramics and some other bioactive glass-ceramics.

Fluorosilicate glass-ceramics are characterized by unique mechanical properties dependent upon highly anisotropic crystals, which assume one- or two-dimensional form. Thus, mica glass-ceramic displays mechanical machineability, whereas glass-ceramic based on amphibole and other chain silicates has shown extreme strength and toughness. Fluorosilicates-containing glass-ceramics are characterized as being less sensitive to superficial damages and exhibit higher thermal shock, erosion and fracture strength than common ceramic

* Corresponding author. Tel.: +20 233371362; fax: +20 233370931; mobile: +20 1146027924.
E-mail address: ha.ebrahim@nrc.sci.eg (H.A. Abo-Mosallam).

Peer review under responsibility of The Ceramic Society of Japan and the Korean Ceramic Society.

http://dx.doi.org/10.1016/j.jascer.2015.04.004

materials [8]. Several noteworthy synthetic glass-ceramics have been developed based on fluorosilicates crystalline phases: potassium fluorphlogopite ($KMg_3AlSi_3O_{10}F_2$), fluorrichterite ($KNaCaMg_5Si_8O_{22}F_2$), fluorcanasite ($(Na,K)_6Ca_5Si_{12}O_{30}F_4$), and fluor-miserite ($KCa_5\square(Si_2O_7)(Si_6O_{15})(OH)F$, where □ denotes a vacancy or "virtual site" within the structure [8]. The miserite crystalline phase, which strengthens glass-ceramic materials, has been described as a pyroxenoid (wollastonite) or hydrous pyroxenoid derivative (pectolite). It is anticipated that miserite glass-ceramic has biocompatibility, bioactivity, and excellent machineability. Thus, miserite glass-ceramic is a promising biomaterial for dental implant applications as an alternative to metallic titanium, due to its biological, mechanical and optical properties [9]. Another interesting fluorine-containing crystalline phase in glass-ceramics is cuspidine ($Ca_4Si_2O_7F_2$), a sorosilicate with isolated $(Si_2O_7)^{6-}$ double tetrahedral groups. Cuspidine is the most abundant high temperature phase in mould fluxes used in continuous casting of steel [10].

In order to enhance the capability of sensitivity of bioglass reactions in vivo, the glass could be doped with a luminescent rare earth (RE). Cerium is known to possess bacteriostatic properties and low toxicity [11]. It has been reported [12] that the activity of cerium (III) sulfadiazine against various microorganisms is comparable to that of silver sulfadiazine and cerium-doped bioactive glasses. It could be useful when implantation concerns with periodontal pockets, infected frontal sinuses, and hypersensitive teeth as a complication of periodontal treatment or tooth wear that has resulted in the exposure of dentine and dental tubules [13].

The main purpose of the present paper is to study the effect of compositional changes on crystallization behaviour and the in vitro bioactivity for a series of glasses based on Na_2O–K_2O–CaO–SiO_2–F glass system with different Na_2O/K_2O replacement ratio. Minor amount of cerium oxide CeO_2 was introduced in the glass formula at the expense of calcium. This work is concerned with the fundamental knowledge for the type of phases, solid solutions, and the microstructure formed in the glass-ceramic materials and their biological behaviour.

2. Materials and methods

The compositions of glasses studied are listed in Table 1. Analytical grade reagents Na_2CO_3, K_2CO_3, $CaCO_3$, CaF_2, CeO_2, and Quartz (SiO_2) were used as starting materials. The homogeneous weighed batch materials (100 g), after thorough mixing, were preheated at 1000 °C for 1 h for calcination and to avoid the volatilization. The melting process was performed in a platinum crucible in a Vecstar electric furnace at 1400–1450 °C for 1.5 h. The melts were then cast into hot stainless steel moulds. The glasses were annealed at 500 °C for 1 h, and then the muffle furnace cooled to room temperature to remove the residual thermal stress.

The thermal behaviour of glasses was monitored by DTA using a differential thermal analyzer (SDTQ 600 – TA Instruments, USA) to know the glass transition (T_g) and crystallization (T_c) temperatures and to determine the optimum conditions for heat treatment processing where the temperature ranges between 25 and 1000 °C. The cast glass was crushed and sieved between 90 and 125 μm to produce glass powder suitable for DTA. About 30 mg powdered sample was placed in an alumina crucible and subjected to a heating rate of 10 °C/min from ambient temperature to 1000 °C in a flowing high purity nitrogen environment.

The progress of crystallization in the glasses was followed using double stage heat-treatment regimes. Crystallization was carried out at temperatures in the region of the main DTA exothermic peak determined for each glass. The glasses were first heated according to the DTA results at the endothermic peak temperature for 5 h, which was followed by another thermal treatment at the exothermic peak temperature for 10 h. To characterize the crystalline phases of glass-ceramic samples after controlled heat treatment, powder XRD was conducted on a diffractometer (PW1080, PANalytics, Netherlands) with Cu Kα radiation (40 kV and 30 mA source). Spectra were obtained from 10° to 80° 2θ at a step size of 0.02°. The JCPDS reference cards were used to interpret the patterns.

The microstructure observation of the glass-ceramic samples was examined using a scanning electron microscope (Quanta FEG 250, Netherlands) equipped with an energy dispersive X-ray spectroscopy (EDX) system. The fracture sample surfaces were chemically etched by immersion in a ($1\%HF + 1\%HNO_3$) aqueous solution for 60 s. After that, the samples were ultrasonically washed with distilled water and dried in the dryer. The fracture surfaces were coated with a thin layer of gold by sputtering method.

In order to estimate the in vitro bioactivity test of the selected glass-ceramic specimens, we used the SBF proposed by Kokubo et al. [14]. The Tris-buffered SBF composition is (Na^+ 142.0, K^+ 5.0, Mg^{2+} 1.5, Ca^{2+} 2.5, Cl^- 147.8, HCO^{3-} 5.0, $HPO_4{}^{2-}$ 1.0 and $SO_4{}^{2-}$ 0.5 mol m^{-3}). The specimens were cut by a low speed diamond disc into rectangular pieces of dimensions (10 mm × 10 mm × 5 mm). The samples were polished and sequentially ultrasonically washed in isopropyl alcohol, in acetone, and in deionized water and then air-dried. These specimens were vertically mounted on a nylon wire in polyethylene falcon test tubes containing 50 ml of SBF for 21 days at 37 ± 0.5 °C and pH = 7.2 ± 0.3, using HCl 0.1 N for pH adjustment. The ratio of the SBF volume to the area of ceramic was equal to 0.5 cm^3 mm^{-2}. After the immersion time the samples were gently rinsed with deionized water and acetone and dried in air at room temperature. The surfaces of dried samples were analyzed by (SEM–EDX) and (FTIR) to detect the appearance of HCA layer. The glass-ceramic samples were analyzed by FTIR-6100 type A machine (The Netherlands). The spectra were obtained between 400 and 1600 cm^{-1} wave number with resolution of 2 cm^{-1}.

3. Results

3.1. Crystallization characteristics

Typical DTA of the glass samples crystallized at the heating rate of 10 °C/min are shown in Fig. 1. The results indicate that the investigated glass has followed the typical behaviour of the vitreous materials transforming into the glass-ceramic. The DTA spectrum of each glass displays the glass transition temperature (T_g) as a shoulder endothermic peak at which the atoms begin to arrange themselves in preliminary structural elements subsequent to crystallization. The crystallization temperature of the glass (T_c), as an exothermic peak indicating crystallization reaction in the glasses, are also recorded. The base glass sample G_1 has a glass transition temperature (T_g) of 705 °C and a crystallization temperature (T_c) of 870 °C. The DTA data reveal that the addition of Na_2O instead of K_2O led to shifting the endothermic dips to lower temperatures, i.e., lower temperature is needed to start the nucleation process in the glasses. In contrast the DTA data (Fig. 1) reveal that the endothermic dips as well as the onset of crystallization were shifted to higher temperature with the addition of CeO_2 at the expense of CaO.

In order to identify the crystalline phase's assemblage in the resultant glass-ceramic formed through crystallization of the studied glasses, each glass was heat treated at its crystallization peak temperatures (extracted from the relevant DTA thermograph) for 10 h. The phases developed in glass-ceramics as indicated by the X-ray diffraction analysis (Figs. 2 and 3) are wollastonite solid solution and pseudo-wollastonite. The X-ray diffraction analysis (XRD) (Fig. 2, pattern I, Table 2) indicated that the base glass (G_1) crystallized at 705 °C/5 h–870 °C/5 h to form only monomineralic

Table 1
The composition and the DTA data of the investigated glasses.

Sample	Oxide constitutions (mol%)						DTA data	
	K_2O	Na_2O	CaO	SiO_2	CaF_2	CeO_2	T_g	T_c
G_1	5.17	–	29.31	55.18	10.34	–	707	871
G_1Ce	5.17	–	28.31	55.18	10.34	1.0	710	894
G_2	3.45	1.72	29.31	55.18	10.34	–	695	858
G_3	1.72	3.45	29.31	55.18	10.34	–	683	846
G_4	0.0	5.17	29.31	55.18	10.34	–	669	817
G_4Ce	0.0	5.17	28.31	55.18	10.34	1.0	676	823

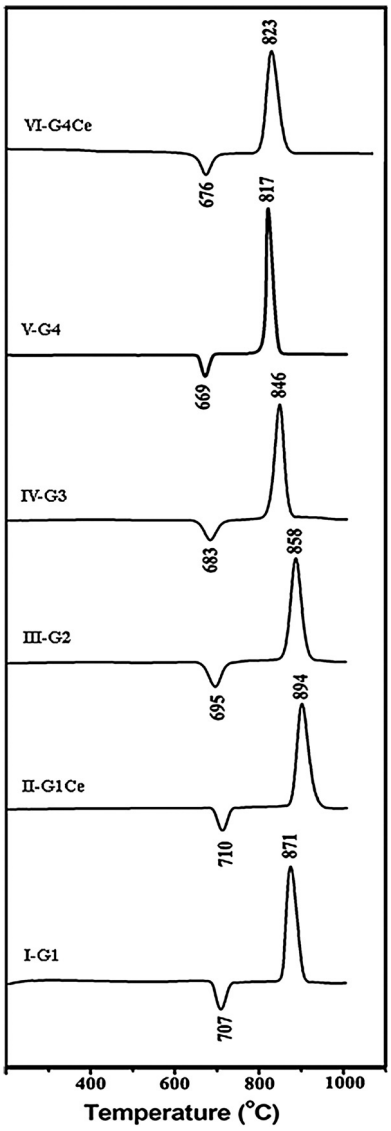

Fig. 1. DTA data of the investigated glasses.

Table 2
Crystalline phases developed and the properties of the investigated glass-ceramic samples.

Sample	Heat treatment (°C/h)	Crystal phases developed
G_1	705/5–870/10	Wollastonite ss 1
G_1Ce	710/5–895/10	Wollastonite ss + pseudo-wollastonite
G_2	695/5–860/10	Wollastonite ss 2
G_3	685/5–845/10	Wollastonite ss 3
G_4	670/5–820/10	Wollastonite ss 4
G_4Ce	675/5–825/10	Wollastonite ss 5

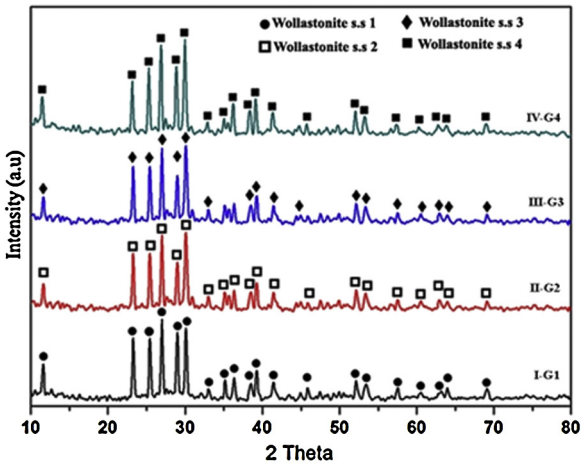

Fig. 2. X-ray diffraction patterns of the crystallized glasses (G_1–G_4).

phase of wollastonite solid solution type (major lines 3.83, 3.49, 3.31, 3.08, 2.98, 2.55 JCPDS, 27-1064). The XRD analysis clearly indicated that the diffraction lines of the solid solution formed were identical, with a slight shift, to those of wollastonite-$CaSiO_3$ (PDF No. 27-1064). The addition of Na_2O instead of K_2O in the glasses i.e., G_2, G_3 and G_4, revealed that the thermal treatment of these glasses at 695 °C/5 h–860 °C/10 h, 685 °C/5 h–845 °C/10 h, and 670 °C/5 h–820 °C/10 h, respectively, led to the formation of wollastonite solid solution phase as confirmed by the XRD analysis (Fig. 2, patterns II–IV).

A detailed study of the effect of CeO_2/CaO replacement on the crystal phase constitution developed in the glass-ceramic materials (G_1Ce and G_4Ce) was obtained by the X-ray diffraction analysis (XRD) (Fig. 3 and Table 2). The addition of CeO_2 instead of CaO in glass G_1 resulted into the crystallization of a

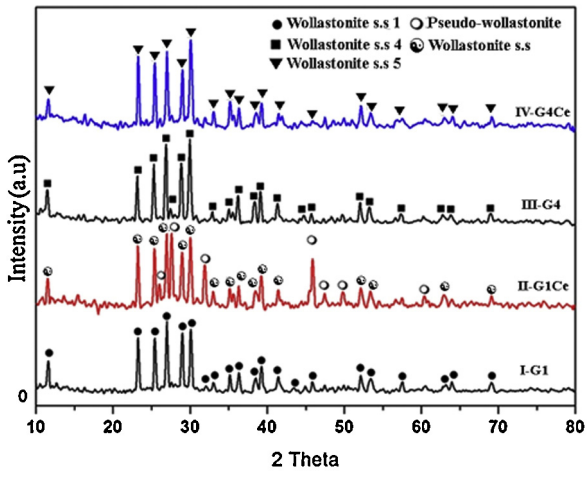

Fig. 3. X-ray diffraction patterns of the crystallized glasses G_1, G_1Ce, G_4 and G_4Ce.

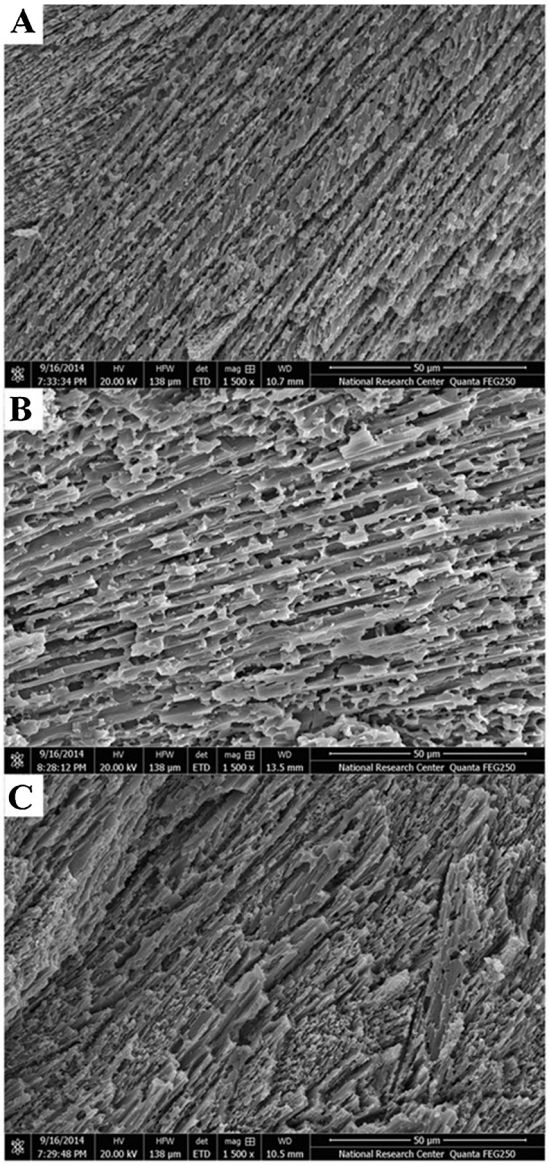

Fig. 4. SEM micrograph of fracture surface of glass-ceramic G_1 (A), G_4 (B), and G_1Ce (C).

pseudo-wollastonite-like phase (major lines 3.42, 3.23, 3.31, 2.90, 1.97 JCPDS, 10-468) together with the wollastonite solid solution (Fig. 3, pattern II). Mineralogically, only wollastonite solid solution phase was formed and no other phases could be detected by the replacement of CaO by CeO_2 in G_4 as indicated from X-ray diffraction analysis (Fig. 3, pattern IV).

Fig. 4 shows the SEM micrograph of the selected glass-ceramic samples obtained by controlled heat-treatment conditions. The microstructure of the base glass-ceramic G_1 (heat treated at 705 °C for 5 h and 870 °C for 10 h) is shown in Fig. 4(A). The rod-shaped grooves due to the detachment of wollastonite solid solution as the only crystalline phase crystallites are clearly observed on the etched fracture surface. The microstructure of the glass-ceramic sample G_4 (heat treated at 670 °C for 5 h and 815 °C for 10 h) is shown in Fig. 4(B). The sample showed similar microstructure as G_1 but with large size. The addition of minor amount of cerium oxide CeO_2 instead of CaO in the base glass led to crystallization of prismatic crystals beside rod-shaped crystals in crystalline sample G_1Ce as shown in Fig. 4(C). The formation of prismatic crystals may be attributed to crystallization of pseudo-wollastonite phase.

3.2. Bioactivity

The in vitro bioactivity of the glass-ceramic samples was investigated by soaking the samples in SBF. SEM images and EDX spectra of the crystalline specimens after 21 days of immersion in the simulated body fluid SBF are presented in Fig. 5. The scanning electron micrographs of the crystalline samples show that surface spherules layers are formed which are assumed to be due to the formation of the apatite phase as revealed by the EDX analysis. This has resulted from the interaction of the glass-ceramic surface with the SBF solution. The EDX analysis of G_1 and G_4 revealed that the presence of Ca, Si, O, P, Na, K and Mg could be found. The presence of Ca, Si, K, Na and O may be attributed to the elemental composition of the glass-ceramic. The presence of P was in an appreciable amount reflecting the bioactivity obtained due to soaking in the SBF solution. The EDX results showed that the Si content decreased significantly while the Ca and P contents increased with Na/K replacement indicating that the layer formed on the G_4 sample surface is rich in calcium and phosphorus layer. The EDX analysis of the surface of crystalline specimen G_1Ce (Fig. 5) revealed that significant peaks of calcium and phosphorous were present while silicon peak disappeared.

Fig. 6 shows the FTIR spectra of the glass-ceramic samples after soaking for 21 days in SBF solution. No significant differences were observed in the FTIR spectra. Phosphate absorption bands at 1025, 620, 578, and 450 cm^{-1} were observed in all samples, where the double peaks at 620 and 578 cm^{-1} were characteristic feature of phosphate in crystalline phases [15]. Carbonate bands at 1423 and 871 cm^{-1} were also detected.

4. Discussion

4.1. Crystallization characteristics

The crystallization is the process by which the regular lattice of the crystals is generated from the less well-ordered liquid structure; it is essentially an ordering phenomenon [16]. The DTA data give evidence that the crystallization characteristics of the glasses were markedly improved by Na_2O/K_2O replacements. The addition of sodium instead of potassium oxide modifies the local structure in glass. We observed that the glass transition temperature T_g tends to shift to lower temperature as the sodium oxide content is increased at the expense of potassium oxide. This could be attributed to the addition of sodium instead of potassium in the glasses that led to decreasing the activation energy of the glass crystallization. On the contrary the addition of K_2O instead of Na_2O in the glasses led to the shift of both the endothermic and exothermic peak temperatures towards higher temperature values, which means that a higher energy is needed to induce crystallization in the thermally treated glass [17]. Glass transition temperature is a characteristic of structural relaxations taking place in the glass network and hence strongly depends on the nature of the structural units constituting the glass network and their connection way. Wang et al. [18] reported that the substitution of K_2O for Na_2O in the glass leads to shifting of glass transition temperatures to higher values, which enhances the thermal stability of the studied glass.

Light rare-earth elements, like Ce^{3+}, La^{3+}, and Pr^{3+}, can readily be substituted for calcium in glasses because their ionic radii are very close to that of Ca^{2+} and the charge balance may be readily maintained with coupled substitutions, such as $2Ca^{2+} = RE^{3+} + Na^{+}$ [19]. The addition of CeO_2 at the expense of CaO led to shifting both the endothermic and exothermic peaks towards higher temperature values, i.e. a higher energy is needed to induce crystallization in the glass. This could be attributed to the ability of CeO_2 to form CeO_4 group, these tetrahedral (CeO_4) structures led to an increase in the viscosity of the glass which hinders the diffusion of different

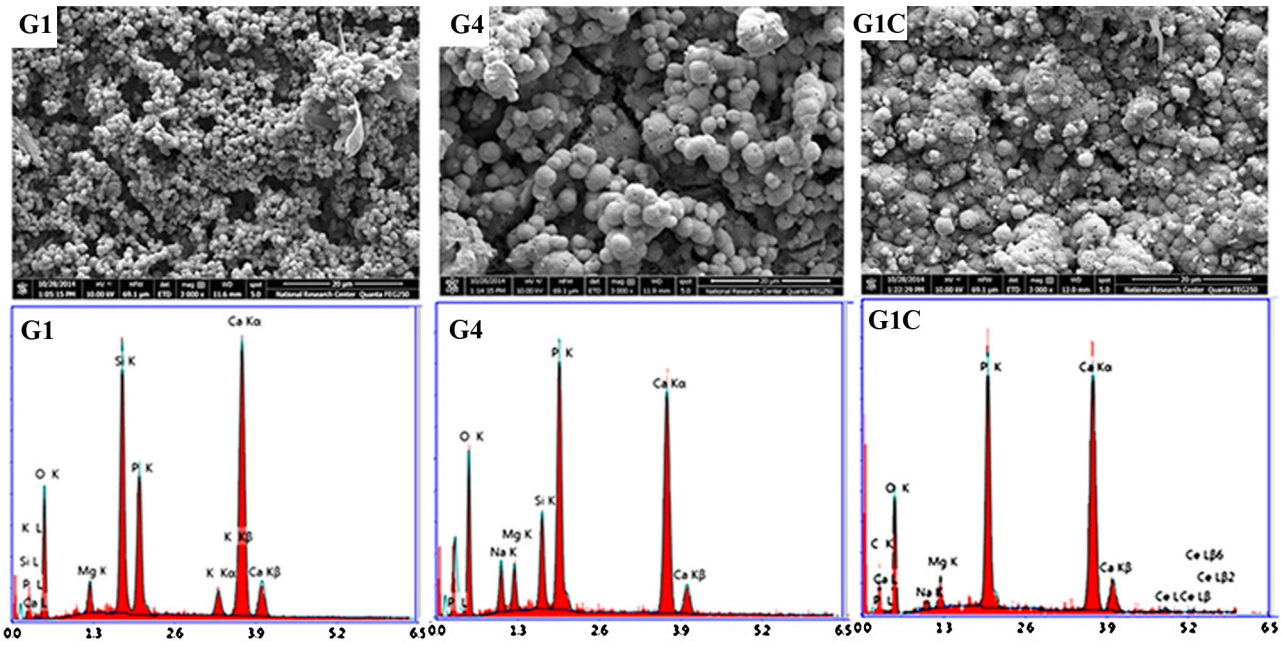

Fig. 5. SEM images and EDX analysis of the crystalline specimens after immersion in SBF solution for 21 days.

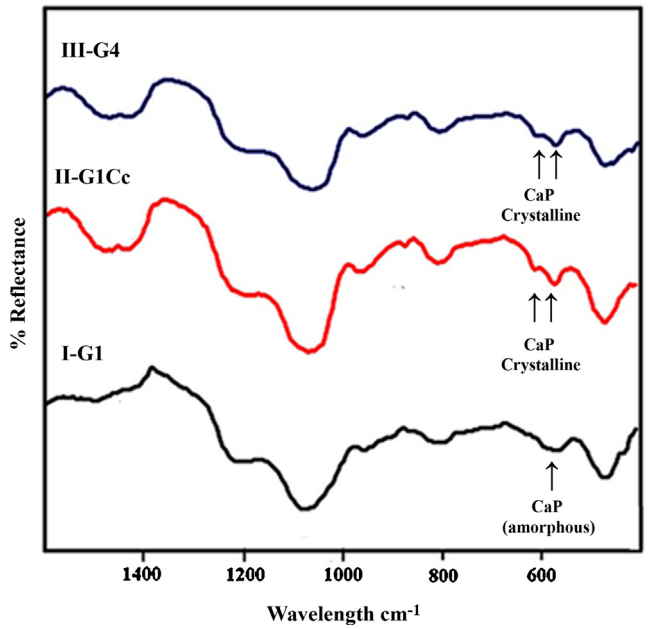

Fig. 6. FTIR of the crystallized samples after immersion in SBF solution for 21 days.

ions and ionic complexes, and consequently, it decreases the rate of crystal growth during the crystallization of the glass resulting in some difficulty in the glass-crystal conversion [20].

Nucleation and crystallization mechanisms used in the development of glass-ceramics are controlled by taking advantage of various solid state reactions. The quantification of the different crystalline phases is indeed important for optimizing the properties of the glass-ceramics. In order to understand and explain the details of crystallization sequence in the most promising glass samples, after subjecting them to controlled heat treatment conditions, they were analyzed by XRD. The conditions of heat treatment and the crystallization products are tabulated in Table 2. The X-ray diffraction analysis revealed that the base glass G_1 crystallized into wollastonite ss phase and no other phases could be detected. The d-spacing reflections of the wollastonite solid solution formed are similar to those characteristics for wollastonite phase. This will lead to an important conclusion that all other elements present in the melt can find place in the wollastonite structure [21]. Casasola et al. [8] obtained similar results in their study on crystallization of glass compositions in the SiO_2–CaO–K_2O–F glass system. They pointed out that internal crystallization of the bulk glass samples favours the formation of wollastonite ss phase. Wollastonite could acquire considerable amounts of Fe^{2+}, Mn^{2+}, Mg^{2+}, K^+, Na^+, etc. replacing Ca^{2+} and Ti^{4+}, and with Ce^{4+} replacing Si^{4+} in its structure [6]. The radius of F^- (1.36 Å) is very close to that of O^{2-} (1.40 Å), so F^- could replace O^{2-} easily. Therefore, double F^- replace an O^{2-} in the glass network structure according to the electrostatic valence equilibrium rules [22]. Theoretically, [23] it is assumed therefore, that the wollastonite ss 1 formed in the glass-ceramic of G_1 has probably the following formula:

$(Ca_{0.79}, K_{0.21})Si(O_{0.88}, F_{0.12})_3$ wollastonitess1

It is well known that compositions crystallizing to give solid solution series are important to control the properties of the resultant materials and offer an excellent opportunity to the glass-ceramic study [1,24]. The present results revealed that predominant wollastonite solid solution phase was developed only from the glass-ceramic materials G_2–G_4. This supports the view that sodium, potassium, and fluorine ions could be incorporated in the wollastonite structure. Theoretically, it is assumed therefore that the wollastonite solid solution phase formed in glass-ceramic of G_2 has probably the following formula:

$(Ca_{0.79}, K_{0.14}, Na_{0.7})Si(O_{0.88}, F_{0.12})_3$ wollastonitess2

As for sample G_3, the replacement of K_2O by Na_2O gave rise to the development of the wollastonite solid solution which has the probable formula of:

$(Ca_{0.79}, K_{0.7}, Na_{0.14})Si(O_{0.88}, F_{0.12})_3$ wollastonitess3

The complete replacement of Na_2O at the expense of K_2O (i.e. sample G_4) results in a wollastonite solid solution expressed by the following formula:

$(Ca_{0.79}, Na_{0.21})Si(O_{0.88}, F_{0.12})_3$ wollastonitess4

The results of this study demonstrate that the partial CeO_2/CaO replacement in the base glasses (i.e., G_1Ce) favours the formation of wollastonite ss together with a pseudo-wollastonite. The activation energy of pseudo-wollastonite is less than that of wollastonite. It follows, therefore, that pseudo-wollastonite is formed during the crystallization of the corresponding glass in the stability field of wollastonite as a transitional stage between glass and the stable variety wollastonite [25]. Previously, it was shown that the incorporation of Sr into $CaSiO_3$ increased the crystal dimension which may be responsible for the phase transition from wollastonite to pseudo-wollastonite-like phase [24,26]. On the other hand, in case of the thermally treated glass G_4Ce, the partial substitution of CeO_2 at the expense of CaO does not lead to the formation of different phases rather than those crystallized in glass G_4. Also no cerium containing phases could be detected. The wollastonite solid solution phase formed in glass-ceramic of G_4Ce has probably the following formula:

$(Ca_{0.79}, Na_{0.21})(Si_{0.98}, Ce_{0.012})(O_{0.88}, F_{0.12})_3$ wollastonitess5

4.2. Bioactivity

The rate of the formation of hydroxyl carbonate apatite (HCA) layer is a measure of bioactivity and HCA formation ability is thought to be a critical factor in facilitating the chemical fixation of biomaterials to bone tissue, and ultimately the in vivo success of the bone grafting material [27]. The mechanism of HCA-like phase formation on the silica base materials in SBF solution can be explained in terms of a chemical reaction taking place between the glass-ceramic materials and the solution [5]. When the materials get in contact with the SBF a partial dissolution occurs producing an ionic exchange of Ca^{2+} for $2H^+$ within the material network leading to the formation of silanol groups on the surface of the glass-ceramics. Later there is a partial dissolution of amorphous silica as SiO_3^{2-}. This fact enhances the creation of crystallization nuclei for the Ca–P phase which can be formed from the high concentration of Ca and P present in the medium.

There was evidence to confirm the formation of apatite layer on the surfaces of crystalline specimens with a different magnitude, which was sought by using the EDX/SEM and FTIR techniques after the soaking in the SBF solution for 21 days. It is clear that the bioactivity of the complete Na_2O/K_2O replacement in the glass-ceramic sample (i.e. G_4) is higher than that of the base glass-ceramic sample G_1, as indicated from the EDX patterns (Fig. 5). EDX spectra revealed that the small peak for Si and the large peak for phosphorus were obtained from the surface of G_4 as compared with spectra obtained from G_1. This may be attributed to the solubility of the glass-ceramic sample which was increased by Na_2O/K_2O replacement. Arcos et al. [28] suggest that the release of activation energy of Si^{4+} is the key to determine biological activity in the biomedical materials. The faster the release rates of Si^{4+}, the lower is the release of activation energy; accordingly, the faster the degradation speed, the higher the biological activity. The formation of the apatite layer on the surface of glass-ceramics was improved by Na_2O/K_2O replacement due to the decrease of chemical durability of the crystallized specimens [17].

There was another evidence that confirms the effect of Na_2O/K_2O replacement on the bioactivity of the glass-ceramic samples by using FTIR technique. Fig. 6 shows the FTIR patterns of G_1 and G_4 glass-ceramics, containing constant amounts of K_2O and Na_2O, respectively, after soaking in SBF for 21 days. FTIR spectra after SBF immersion showed single peak or a split peak at approximately 570 cm^{-1}. This is the most characteristic region for apatite and other phosphates, and it corresponds to P—O bonding vibrations in a PO_3^{4-} tetrahedron and indicates the presence of crystalline calcium phosphates including hydroxyl apatite (HA) and hydroxyl carbonate apatite (HCA). A single peak in this region in G_1 crystalline sample explains the formation of non-apatitic or amorphous calcium phosphate (ACP), which is usually taken as an indication of the presence of precursors to hydroxyapatite [29]. Whereas, the split of the peak in G_4 sample at 572 and 608 cm^{-1} is related to the presence of crystalline phosphate [30].

The addition of CeO_2 at the expense of CaO in the G_1 sample (i.e. G_1Ce) showed a positive effect on the bioactivity behaviour of the crystallized samples in the (SBF) solution. This may be attributed to the presence of CeO_2 in the glasses which facilitates the formation of high temperature form of $CaSiO_3$ (pseudo-wollastonite) together with low temperature form (wollastonite). Pseudo-wollastonite ($CaSiO_3$), the high temperature form of wollastonite, displays in its structure calcium ion chains that are easily removed by protons, as Bailey and Reesman [31] showed it in their study of kinetics of dissolution of the wollastonite in H_2O–CO_2 systems. This fact suggests the possibility of extraction of calcium ions, from the wollastonite structure, by protons from the SBF and therefore facilitates the precipitation and formation of the HA layer on the surface of the material. Sainz et al. [32] demonstrate that the pseudo-wollastonite is significantly more soluble in SBF than low temperature wollastonite form $CaSiO_3$. Pseudo-wollastonite contains needle-like structures with significant Ca and Si ions content that favours the formation of an apatite layer on the surface of the wollastonite sample [33].

5. Conclusions

Bioglass-ceramic materials were successfully produced by studying the effects of Na_2O/K_2O and CeO_2/CaO on crystallization behaviour and bioactivity of the K_2O–CaO–SiO_2–F glass system. The glass crystallization temperatures were shifted to lower temperatures as the amount of Na_2O/K_2O replacement was increased. On the contrary, the replacement of the calcium by cerium led to a slight increase in crystallization temperatures. The XRD indicated that the main crystalline phases were wollastonite solid solution and pseudo-wollastonite. The appearance of apatite layer in in vitro test on the surface of glass-ceramics demonstrates the crystalline materials have good bioactivity. The obtained data indicate that the Na_2O/K_2O replacements stimulate the rate of samples dissolution and thus the formation of apatite layer. The results obtained show also that the appearance of pseudo-wollastonite phase works to increase the bioactivity rate of the glass-ceramic formed.

References

[1] W. Höland and G.H. Beall, Glass-Ceramic Technology, 2nd ed., John Wiley & Sons, Inc., Hoboken, NJ (2012).
[2] K.A. Gross and C.C. Berndt, Rev. Miner. Geochem., 48, 631–672 (2002).
[3] L. Hench, J. Am. Ceram. Soc., 74, 1487–1510 (1993).
[4] D.F. Williams, Biomaterials, 30, 5897–5909 (2009).
[5] P.N. De Aza, Z.B. Luklinsk, M.R. Anseau, M. Hector, F. Guitian and S. De Aza, Biomaterials, 21, 1735–1741 (2000).
[6] W.A. Deer, R.A. Howie and J. Zussman, An Introduction to the Rock-forming Minerals, 2nd ed., Longman, London (1992).
[7] P. Siriphannon, S. Hayashi, A. Yasumori and K. Okada, J. Mater. Res., 14, 529–536 (1999).
[8] R. Casasola, J.M. Pérez and M. Romero, J. Non-Cryst. Solids, 378, 25–33 (2013).
[9] S.A. Saadaldin, S.J. Dixon, D.O. Costa and A.S. Rizkalla, Dent. Mater., 29, 645–655 (2013).
[10] A. Cruz, F. Chávez, A. Romero, E. Palacios and V. Arredondo, J. Mater. Process. Technol., 182, 358–362 (2007).
[11] C. Leonelli, G. Lusvardi, G. Malavasi, L. Menabue and M. Tonelli, J. Non-Cryst. Solids, 316, 198–216 (2003).

[12] C.L. Fox, S. Modak, J.W. Stanford and P.L. Fox, Scand. J. Plast. Reconstr. Surg., 13, 89–94 (1979).
[13] P. Stoor, E. Söderling and J.I. Salonen, Acta Odontol. Scand., 56, 161–165 (1998).
[14] T. Kokubo, H. Kushitani, S. Sakka, T. Kitsugi and T. Yamamuro, J. Biomed. Mater. Res., 24, 721–734 (1990).
[15] P. Li, C. Ohtsuki, T. Kokubo, K. Nakanishi, N. Soga, T. Nakamura and T. Yamamuro, J. Mater. Sci. Mater. Med., 4, 127–131 (1993).
[16] P.W. McMillan, Glass-Ceramics, 2nd ed., Academic Press, New York (1979).
[17] S.M. Salman, S.N. Salama and H.A. Abo-Mosallam, Ceram. Int., 38, 55–63 (2012).
[18] F. Wang, Q. Liao, G. Xiang and S. Pan, J. Mol. Struct., 1060, 176–181 (2014).
[19] L.R. Pinckney, G.H. Beall and R.L. Andru, J. Am. Ceram. Soc., 82, 2523–2528 (1999).
[20] Y. Ivanova, J. Spassova, P. Kashchieva, A. Bursukova and B. Dimitiev, J. Non-Cryst. Solids, 192–193, 674–678 (1995).
[21] G. Agarwal, K.S. Hong, M.R. Fletcher and R.F. Speyer, J. Non-Cryst. Solids, 130, 187–197 (1991).
[22] R.M. Atiar and J.B. Bikram, J. Mater. Sci. Mater. Med., 20, 869–882 (2009).
[23] T.F. Barth, Theoretical Petrology, 2nd ed., John Wiley & Sons, Inc., New York (1962).
[24] C.T. Wu and H. Zreiqat, Key Eng. Mater., 302–332, 499–502 (2007).
[25] A.A. Omar and S.M. Salman, Cent. Glass-Ceram. Bull., 18, 32–36 (1971).
[26] S.M. Salman, S.N. Salama and E.A. Mahdy, Ceram. Int., 41, 137–143 (2015).
[27] M.R. Filgueiras, G. La Torre and L.L. Hench, J. Biomed. Mater. Res., 27, 445–453 (1993).
[28] D. Arcos, D.C. Greenspan and M. Vallet-Regí, J. Biomed. Mater. Res. Part A, 65, 344–351 (2003).
[29] J.R. Jones, P. Sepulveda and L.L. Hench, J. Biomed. Mater. Res., 58, 720–726 (2001).
[30] H.C. Li, D.G. Wang, J.H. Hu and C.Z. Chen, J. Colloid Interface Sci., 405, 296–304 (2013).
[31] A. Bailey and A.L. Reesman, Am. J. Sci., 271, 464–472 (1971).
[32] M.A. Sainz, P. Pena, S. Serena and A. Caballero, Acta Biomater., 6, 2797–2807 (2010).
[33] R. Abd Rashid, R. Shamsudinn, M.A. Abdul Hamid and A. Jalar, Ceram. Int., 40, 6847–6853 (2014).